

# Engineering Notes

## Decentralized Robust Adaptive Control for Attitude Synchronization Under Directed Communication Topology

Baolin Wu\* and Danwei Wang†

Nanyang Technological University,  
 Singapore 639798, Republic of Singapore  
 and  
 Eng Kee Poh  
 DSO National Laboratories,  
 Singapore 118230, Republic of Singapore

DOI: 10.2514/1.50189

### I. Introduction

THE need to maintain accurate relative orientation between spacecraft is critical in many satellite formation missions. For instance, in interferometry application, the relative orientation between spacecraft in a formation is required to be maintained precisely during formation maneuvers. In interspacecraft laser communication operation, the participating spacecraft are also required to maintain accurate relative attitude throughout the communication process. This control problem, commonly referred to as attitude synchronization in the literature, has attracted much research attention. Various solutions have been proposed and these can be broadly classified according to the advocated techniques: leader–follower [1–4], virtual structure [5,6], behavior-based [7–11], and graph-theoretical approach [12–15].

In particular, the graph-theoretical approach has been actively studied for cooperative control of multi-agent system using limited local interaction [16,17] and was adopted for attitude synchronization problem in [12–15]. In the above-cited decentralized attitude synchronization results, except [14,15], it is assumed that the interspacecraft communication links are undirected (i.e. bidirectional). However, in practice, the interspacecraft communication topology may be restricted to be directed, such as in unidirectional satellite laser communication system. The control problem of attitude synchronization under directed communication topology is more challenging as compared with the case with undirected communication topology. This issue was studied in [14] but the proposed control law requires derivative of the angular velocity, which may introduce additional noise into the system. Furthermore, the attitude-tracking performance analysis in [14] is applicable only to the case where the directed graph can be simplified to a graph with only one node. This constraint on communication topology is relaxed in [15], which uses modified Rodriguez parameters and Euler–Lagrange system to describe the satellite attitude dynamics. However, modified Rodriguez parameters contain singularity and are

Received 5 April 2010; revision received 28 December 2010; accepted for publication 30 January 2011. Copyright © 2011 by the American Institute of Aeronautics and Astronautics, Inc. All rights reserved. Copies of this paper may be made for personal or internal use, on condition that the copier pay the \$10.00 per-copy fee to the Copyright Clearance Center, Inc., 222 Rosewood Drive, Danvers, MA 01923; include the code 0731-5090/11 and \$10.00 in correspondence with the CCC.

\*Ph.D. Student; wubaolin83@gmail.com.

†Professor, School of Electrical and Electronics Engineering, Nanyang Avenue; edwwang@ntu.edu.sg (Corresponding Author).

thus not suitable for the development of globally stabilizing control algorithms.

This Note proposes a decentralized adaptive sliding-mode control law which regulates attitude and angular velocity errors of individual spacecraft with respect to reference commands and minimizes relative attitude and angular velocity errors between spacecraft. Thus, the proposed control law ensures that each spacecraft attains desired time-varying attitude and angular velocity while maintaining attitude synchronization with other spacecraft in the formation even in the presence of model uncertainties and external disturbances. Moreover, the design is applicable to general communication topology and is not restricted to ring topology or undirected communication topology.

In the following section, unit quaternion representation will be introduced into the satellite attitude control problem and algebraic graph theory will be applied to describe general directed communication topology.

### II. Attitude Dynamics and Mathematical Preliminaries

#### A. Spacecraft Attitude Dynamics

The rigid spacecraft attitude-tracking error dynamics is described as follows [18]:

$$\begin{aligned} J_i \dot{\tilde{\omega}}_i &= -\omega_i^{\times} J_i \omega_i + J_i (\tilde{\omega}_i^{\times} R(\tilde{q}_i) \omega_i^d - R(\tilde{q}_i) \dot{\omega}_i^d) \\ &+ u_i + z_i, \quad i = 1, \dots, n \end{aligned} \quad (1)$$

$$\dot{q}_i = \frac{1}{2} (q_i^{\times} + q_{0,i} I) \tilde{\omega}_i, \quad i = 1, \dots, n \quad (2)$$

$$\dot{q}_{0,i} = -\frac{1}{2} q_i^T \tilde{\omega}_i, \quad i = 1, \dots, n \quad (3)$$

where superscript  $i$  denotes the  $i$ th spacecraft in the formation,  $\omega_i^d \in \mathbb{R}^3$  denotes the desired angular velocity of the  $i$ th spacecraft with respect to the inertial frame  $I$ . In addition,  $\omega_i \in \mathbb{R}^3$  denotes the body angular velocity of the  $i$ th spacecraft with respect to an inertial frame  $I$ ,  $\tilde{\omega}_i = \omega_i - R(\tilde{q}_i) \omega_i^d$  denotes the angular velocity error,  $R(\tilde{q}_i)$  is the rotation matrix from the  $i$ th spacecraft's reference frame to its body-fixed frame,  $q_i \in \mathbb{R}^3$  and  $q_{0,i} \in \mathbb{R}$  denote the vector part and scalar part of error quaternion, respectively,  $z_i \in \mathbb{R}^3$  denotes the disturbance torque,  $u_i \in \mathbb{R}^3$  denotes the control torque,  $I$  denotes the  $3 \times 3$  identity matrix,  $J_i \in \mathbb{R}^{3 \times 3}$  denotes the inertia matrix, The notation  $a^{\times}$  for a vector  $a = [a_1 \ a_2 \ a_3]^T$  is used to denote the following skew-symmetric matrix:

$$a^{\times} = \begin{bmatrix} 0 & -a_3 & a_2 \\ a_3 & 0 & -a_1 \\ -a_2 & a_1 & 0 \end{bmatrix}$$

It can be seen from Eqs. (1–3) that the spacecraft attitude-tracking problem is equivalent to an asymptotic stabilization problem for  $\tilde{\omega}_i$  and  $q_i$ .

#### B. Algebraic Graph Theory

The necessary results from algebraic graph theory are introduced in this section to address the decentralized cooperative attitude synchronization problem using a general directed communication topology. A directed communication topology can be described by directed graph. A directed graph  $G_n$  consists of a finite set of vertices, denoted  $V$ , and a set of arcs  $A \subset V^2$ , where  $a = (\alpha, \beta) \in A$  and  $\alpha, \beta \in V$ . The arc  $(\alpha, \beta)$  denotes that vertex  $\beta$  can obtain the information of vertex  $\alpha$ . In spacecraft attitude synchronization

application, the arc  $(\alpha, \beta)$  denotes spacecraft  $\beta$  can obtain attitude information of spacecraft  $\alpha$ . It is assumed that the graph has no self-loops, meaning that  $(\alpha, \beta) \in \mathbf{A}$  implies  $\alpha \neq \beta$ . The adjacency matrix of  $G_n$ , denoted  $A$  is a square matrix of size  $n$  with entries

$$\begin{cases} a_{i,j} > 0 & \text{if } (\alpha_j, \alpha_i) \in \mathbf{A} \\ a_{i,j} = 0 & \text{otherwise} \end{cases} \quad (\alpha_i, \alpha_j \in \mathbf{V}) \quad (4)$$

where the nonnegative  $a_{i,j}$  is subsequently chosen to be the control weight parameter for attitude synchronization between the  $i$ th and  $j$ th spacecraft. Note that  $a_{i,i} = 0$  from Eq. (4).

The in-degree matrix of  $G_n$  is the diagonal matrix  $D$  with diagonal entries

$$d_{i,i} = \sum_{j=1, j \neq i}^n a_{i,j}, \quad i = 1, \dots, n \quad (5)$$

Following [19], the Laplacian  $L \in \mathbb{R}^{n \times n}$  of the graph  $G_n$  is defined as

$$L = D - A \quad (6)$$

Note that a graph with the property that for any  $(\alpha, \beta) \in \mathbf{A}$ , the arc  $(\beta, \alpha) \in \mathbf{A}$  as well is said to be undirected. In spacecraft attitude synchronization application, this corresponds to having bidirectional measurement. It is valid to assume  $a_{i,j} = a_{j,i}$  in the case of the undirected communication topology. Under this assumption, the Laplacian  $L$  is a symmetrical matrix, which simplifies the stability analysis of cooperative control system. However, in the case of directed communication topology,  $L$  is generally not symmetric because  $a_{i,j} = a_{j,i}$  does not hold.

The following results will be used in Sec. III to derive stability proof for the proposed controller design.

*Lemma 1* [19]: For a directed graph  $G_n$  with  $N$  vertices, all the eigenvalues of the weighted Laplacian  $L$  have a nonnegative real part (follows from Gershgorin's theorem).

*Lemma 2* [20]: Suppose that  $M \in \mathbb{R}^{m \times m}$ ,  $N \in \mathbb{R}^{n \times n}$ ,  $X \in \mathbb{R}^{m \times m}$ , and  $Y \in \mathbb{R}^{n \times n}$ . The following results hold:

1)  $(M \otimes N)(X \otimes Y) = MX \otimes NY$ , where  $\otimes$  denotes the Kronecker product.

2) Suppose that  $M$  and  $N$  are invertible. Then  $(M \otimes N)^{-1} = M^{-1} \otimes N^{-1}$ .

3) Let  $\lambda_1, \dots, \lambda_m$  be the eigenvalues of  $M$  and  $\mu_1, \dots, \mu_n$  be those of  $N$ . Then the eigenvalues of  $M \otimes N$  are  $\lambda_i \mu_j$  ( $i = 1, \dots, m$  and  $j = 1, \dots, n$ ).

### III. Robust Adaptive Control Law Design for Attitude Synchronization and Tracking

In this section, a decentralized adaptive sliding-mode control law is proposed for attitude synchronization and tracking using a general directed communication topology. Firstly, the multispacecraft sliding-mode vector is developed. Subsequently, a decentralized adaptive sliding-mode control law is derived based on the multispacecraft sliding-mode vector.

The following assumptions are made about the dynamics of the attitude synchronization and tracking systems

*Assumption 1:* Let  $J_i = \bar{J}_i + \Delta J_i$ , where  $\bar{J}_i$  and  $\Delta J_i$  are the nominal part and uncertain part of the inertia matrix of the  $i$ th spacecraft, respectively. The inertia matrix uncertainty  $\Delta J_i$  is assumed to satisfy  $\|\Delta J_i\| \leq \gamma_i$ .

*Assumption 2:* The desired angular velocity of spacecraft with respect to the inertial frame  $I$ , denoted by  $\omega_i^d$ , and its time derivative  $\dot{\omega}_i^d$  are assumed to be bounded;

*Assumption 3:* All the environmental disturbances due to gravitation, solar radiation pressure, magnetic forces and aerodynamic drag are assumed to be bounded. Thus, the external disturbances  $z_i$  are assumed to satisfy  $\|z_i\| \leq \gamma_i$ ;

*Assumption 4:* The control law of each spacecraft might use angular velocity errors and error quaternions of its neighboring spacecraft in the cooperative attitude control problem, and error quaternion is bounded from its definition. Thus, the control torque  $u_i$  is assumed to satisfy

$$\|u_i\| \leq \xi_{i,0} + \xi_{i,1} \sum_{j \in N_i} \|\tilde{\omega}_j\| + \xi_{i,2} \sum_{j \in N_i} \|\tilde{\omega}_j\|^2$$

where  $\gamma_i$  and  $\xi_{i,j}$  ( $i = 1, \dots, n, j = 0, 1, 2$ ) are unknown nonnegative constant,  $N_i$  denotes the  $i$ th spacecraft and all spacecraft with which the  $i$ th spacecraft can communicate, and  $\|\cdot\|$  denotes the standard Euclidean vector norm or induced matrix norm, as appropriate.

#### A. Multispacecraft Sliding Manifold

In this subsection, the multispacecraft sliding-mode vector is developed in order to guarantee attitude synchronization and tracking in spacecraft formation and is defined as

$$S = [s_1, \dots, s_n]^T \quad (7)$$

where  $s_i \in \mathbb{R}^{3 \times 1}$  is given by

$$\begin{aligned} s_i = b_i \bar{J}_i (\tilde{\omega}_i + C q_i) + \sum_{j=1, j \neq i}^n a_{ij} [(\bar{J}_i \tilde{\omega}_i - \bar{J}_j \tilde{\omega}_j) \\ + (\bar{J}_i C q_i - \bar{J}_j C q_j)], \quad i = 1, \dots, n \end{aligned} \quad (8)$$

with  $C$  being a positive definite constant matrix, scalar  $b_i > 0$  is the control weight parameter for attitude tracking of the  $i$ th spacecraft (station-keeping behavior), scalar  $a_{ij} \geq 0$  defined in is the control weight parameter for interspacecraft attitude synchronization between the  $i$ th and  $j$ th spacecraft (formation-keeping behavior) and  $\bar{J}_i$  is the nominal inertia matrix of the  $i$ th spacecraft.

*Remark 1:* In the case of undirected communication topology, it is valid to assume  $a_{i,j} = a_{j,i}$  in Eq. (8). This assumption greatly simplifies the stability proof of the cooperative attitude control system, because some terms involving  $a_{i,j}$  in the time derivative of the Lyapunov function are eliminated by mutual cancellation. However, it is not valid to assume  $a_{i,j} = a_{j,i}$  in the case of directed communication topology. Thus, cooperative control for attitude synchronization under directed communication topology is more challenging as compared with the case of undirected communication topology.

Using the Kronecker product, the multispacecraft sliding vector (7) can be rewritten as

$$S = [(L + B) \otimes I_3] \bar{J} (\tilde{\Omega} + \tilde{C} Q) \quad (9)$$

where  $\tilde{\Omega} = [\tilde{\omega}_1, \dots, \tilde{\omega}_n]^T$ ,  $Q = [q_1, \dots, q_n]^T$ ,  $B = \text{diag}[b_1, \dots, b_n]$ ,  $\tilde{C} = \text{diag}[C, \dots, C] \in \mathbb{R}^{3n \times 3n}$ ,  $L$  is the weighted Laplacian matrix corresponding to the interspacecraft directed communication topology as described in Eq. (6), and  $\bar{J} = \text{diag}[\bar{J}_1, \dots, \bar{J}_n]$ .

The multispacecraft sliding-mode surface is then defined as  $S = 0$ . In view of Lemma 1, result 3 in Lemma 2, and the definition of  $B$ , it follows that  $(L + B) \otimes I_3$  has full rank. Furthermore,  $\bar{J}$  has full rank. Consequently,  $[(L + B) \otimes I_3] \bar{J}$  has full rank. Thus, it follows that  $\tilde{\Omega} + \tilde{C} Q = 0$  on the sliding-mode surface  $S = 0$  from Eq. (9).

$\tilde{\Omega} + \tilde{C} Q = 0$  implies  $\tilde{\omega}_i + C q_i = 0$  ( $i = 1, \dots, n$ ). It is obvious that  $\tilde{\omega}_i + C q_i = 0$  implies that

$$\lim_{t \rightarrow \infty} \|\tilde{\omega}_i\| = \lim_{t \rightarrow \infty} \|q_i\| = 0, \quad i = 1, \dots, n \quad (10)$$

It can be concluded that on the multispacecraft sliding-mode surface  $S = 0$ , the attitude error and angular velocity error of each spacecraft will approach zero as  $t \rightarrow \infty$ .

#### B. Decentralized Adaptive Sliding-Mode Control Design

This subsection presents the adaptive sliding-mode control law which ensures that the spacecraft attitude error dynamics (1–3) will converge to the sliding manifold  $S = 0$ .

To develop the control law, the following equations are derived from Eqs. (1) and (2):

$$\bar{J}_i (\dot{\tilde{\omega}}_i + C \dot{q}_i) = h_i + \rho_i + u_i, \quad i = 1, \dots, n \quad (11)$$

with

$$h_i(t) \triangleq -\omega_i^x \bar{J}_i \omega_i + \bar{J}_i (\tilde{\omega}_i^x R(\bar{q}_i) \omega_i^d - R(\bar{q}_i) \dot{\omega}_i^d) + \frac{1}{2} \bar{J}_i C(q_i^x + q_{i,0} I) \tilde{\omega}_i \quad (12)$$

$$\rho_i(t) \triangleq z_i - \Delta J_i \dot{\tilde{\omega}}_i - \omega_i^x \Delta J_i \omega_i + \Delta J_i (\tilde{\omega}_i^x R(\bar{q}_i) \omega_i^d - R(\bar{q}_i) \dot{\omega}_i^d) \quad (13)$$

where  $\rho_i(t)$  represents the inertia matrix uncertainties and external disturbances. Under Assumptions 1–4 and the definition of  $L$  and  $B$ , it can be shown that

$$\|(L + B) \otimes I_3\|_1 \|\rho_i(t)\|_1 \leq c_{i,0} + c_{i,1} \sum_{j \in N_i} \|\tilde{\omega}_j\|_1 + c_{i,2} \sum_{j \in N_i} \|\tilde{\omega}_j\|_1^2 \quad (14)$$

where  $c_{i,0}$ ,  $c_{i,1}$ , and  $c_{i,2}$  are nonnegative constant numbers.

However, in the conventional sliding-mode control laws for attitude control in [18,21,22], an important assumption is that inertia uncertainties and external disturbances are bounded and that their bounds are known to the designer. Typically, bounds on the uncertainties and external disturbances of spacecraft are not available. The implementation of the control law, based on a conservative bound, may result in impractically large control authority and control chattering. Therefore, in order to avoid the requirement of prior knowledge of the upper bound of  $\|(L + B) \otimes I_3\|_1 \|\rho_i(t)\|_1$ , an adaptive mechanism is introduced to estimate its upper-bound parameters.

Let  $\hat{c}_{i,0}$ ,  $\hat{c}_{i,1}$ , and  $\hat{c}_{i,2}$  denote the estimates of  $c_{i,0}$ ,  $c_{i,1}$ , and  $c_{i,2}$ , respectively. Now consider the simple adaptation laws for the upper bound of the norm  $\|(L + B) \otimes I_3\|_1 \|\rho_i(t)\|_1$  such that

$$\begin{aligned} \dot{\hat{c}}_{i,0} &\triangleq \kappa_{i,0} \|s_i\|_1 & \dot{\hat{c}}_{i,1} &\triangleq \kappa_{i,1} \|s_i\|_1 \sum_{j \in N_i} \|\tilde{\omega}_j\|_1 \\ \dot{\hat{c}}_{i,2} &\triangleq \kappa_{i,2} \|s_i\|_1 \sum_{j \in N_i} \|\tilde{\omega}_j\|_1^2 \end{aligned} \quad (15)$$

where  $\tilde{c}_{i,0} = \hat{c}_{i,0} - c_{i,0}$ ,  $\tilde{c}_{i,1} = \hat{c}_{i,1} - c_{i,1}$ , and  $\tilde{c}_{i,2} = \hat{c}_{i,2} - c_{i,2}$  are parameter adaptation errors,  $\kappa_{i,0}$ ,  $\kappa_{i,1}$ , and  $\kappa_{i,2}$  are positive adaptive gains, and  $s_i$  is the component of multispacecraft sliding-mode vector  $S$ , which is defined in Eq. (8).

The control input  $u_i \in \mathbb{R}^{3 \times 1}$  for the  $i$ th spacecraft is proposed as

$$u_i = -h_i + \left( \sum_{j=1, j \neq i}^n a_{ij} + b_i \right)^{-1} \left[ \sum_{j=1, j \neq i}^n a_{ij} (u_j + h_j) - K_i s_i - \hat{\beta}_i \text{sgn}(s_i) \right], \quad i = 1, \dots, n \quad (16)$$

where  $h_i$  is defined in Eq. (12),  $K_i \in \mathbb{R}^{3 \times 3}$  is a positive definite gain matrix,  $a_{ij}$  and  $b_i$  are defined in Eq. (8),  $\text{sgn}(s_i) \triangleq [\text{sgn}(s_{i,1}) \text{sgn}(s_{i,2}) \text{sgn}(s_{i,3})]^T$ ,  $s_{i,j}$  ( $j = 1, 2, 3$ ) is the  $j$ th component of  $s_i$ ,  $\text{sgn}(\cdot)$  denotes the sign function, i.e.,

$$\text{sgn}(x) = \begin{cases} 1, & x > 0 \\ 0, & x = 0 \\ -1, & x < 0 \end{cases}$$

and  $\hat{\beta}_i$  is the adaptive upper bound of the norm  $\|(L + B) \otimes I_3\|_1 \|\rho_i(t)\|_1$  and is defined by

$$\hat{\beta}_i \triangleq \hat{c}_{i,0} + \hat{c}_{i,1} \sum_{j \in N_i} \|\tilde{\omega}_j\|_1 + \hat{c}_{i,2} \sum_{j \in N_i} \|\tilde{\omega}_j\|_1^2, \quad i = 1, \dots, n \quad (17)$$

Note that in the proposed control law (16), the information flow between spacecraft includes the absolute inertial attitude and angular velocity, the desired attitude and angular velocity, and control input, as well as the nominal inertia matrix. Each spacecraft also need to know its own absolute inertial attitude and angular velocity, its own desired attitude and angular velocity, and its own nominal inertia

matrix. Quaternion error and angular velocity error in Eq. (16) can be calculated by using the absolute inertial attitude and angular velocity, as well as the desired attitude and angular velocity. If the desired attitude and angular velocity for each spacecraft are identical, then these two terms are not included in the information flow. Compared with [8], the information flow between spacecraft for the proposed control law includes two more items: the control input and the nominal inertia matrix.

The following theorem establishes the condition for the existence of the multispacecraft sliding-mode surface  $S = 0$  for spacecraft formation attitude-tracking systems described by Eqs. (1–3).

**Theorem 1:** Consider the spacecraft formation attitude-tracking dynamics described by Eqs. (1–3) with the decentralized adaptive sliding-mode control law (16) and the adaptation law (15). If the Assumptions 1–4 are valid, then the multispacecraft sliding-mode surface  $S = 0$  defined in Eq. (7) will be reached asymptotically.

*Proof:* The candidate Lyapunov function is chosen as

$$V = V_1 + V_2 \quad (18)$$

with

$$V_1 = \frac{1}{2} S^T S \quad V_2 = \frac{1}{2} \sum_{i=1}^n (\kappa_{i,0}^{-1} \tilde{c}_{i,0}^2 + \kappa_{i,1}^{-1} \tilde{c}_{i,1}^2 + \kappa_{i,2}^{-1} \tilde{c}_{i,2}^2)$$

Using the Kronecker product and the definition of adjacent matrix  $A$  and in-degree matrix  $D$  of interspacecraft communication graph, Eq. (16) can be rewritten as

$$U = -H + [(D + B)^{-1} \otimes I_3][(A \otimes I_3)(U + H) - \mathbf{K}S - \hat{\beta} \text{sgn}(S)] \quad (19)$$

where  $U = [u_1, \dots, u_n]^T$ ,  $H = [h_1, \dots, h_n]^T$ ,  $\mathbf{K} = \text{diag}[K_1, \dots, K_n]$  and  $\hat{\beta} = \text{diag}[\hat{\beta}_1 I_3, \dots, \hat{\beta}_n I_3]$ .

The above equation can be rewritten as

$$\begin{aligned} U &= -H - \{I_{3n} - [(D + B)^{-1} \otimes I_3](A \otimes I_3)\}^{-1} \\ &\quad \times [(D + B)^{-1} \otimes I_3](\mathbf{K}S + \hat{\beta} \text{sgn}(S)) \\ &= -H - [(L + B) \otimes I_3]^{-1}(\mathbf{K}S + \hat{\beta} \text{sgn}(S)) \end{aligned} \quad (20)$$

where the following equality is used:

$$\begin{aligned} I_{3n} - [(D + B)^{-1} \otimes I_3](A \otimes I_3) &= [(D + B)^{-1} \otimes I_3]\{[(D + B) \otimes I_3] - A \otimes I_3\} \\ &= [(D + B)^{-1} \otimes I_3][(L + B) \otimes I_3] \end{aligned} \quad (21)$$

Taking the first derivative of  $V_1$  and using Eqs. (9) and (11) leads to

$$\begin{aligned} \dot{V}_1 &= S^T \dot{S} = S^T [(L + B) \otimes I_3] (\bar{\mathbf{J}} \dot{\Omega} + \bar{\mathbf{J}} \tilde{\mathbf{C}} \dot{Q}) \\ &= S^T [(L + B) \otimes I_3] (H + \rho + U) \end{aligned} \quad (22)$$

where  $\rho = [\rho_1, \dots, \rho_n]^T$ .

Substituting Eq. (20) into the above equation yields

$$\begin{aligned} \dot{V}_1 &= S^T [(L + B) \otimes I_3] \rho - S^T \hat{\beta} \text{sgn}(S) - S^T \mathbf{K}S \\ &\leq \sum_{i=1}^n (-s_i^T K_i s_i - \hat{\beta}_i \|s_i\|_1 + \|(L + B) \otimes I_3\|_1 \cdot \|\rho_i\|_1 \cdot \|s_i\|_1) \\ &\leq \sum_{i=1}^n \left[ -s_i^T K_i s_i - \left( \hat{c}_{i,0} + \hat{c}_{i,1} \sum_{j \in N_i} \|\tilde{\omega}_j\|_1 + \hat{c}_{i,2} \sum_{j \in N_i} \|\tilde{\omega}_j\|_1^2 \right) \|s_i\|_1 \right. \\ &\quad \left. + \|s_i\|_1 \cdot \left( c_{i,0} + c_{i,1} \sum_{j \in N_i} \|\tilde{\omega}_j\|_1 + c_{i,2} \sum_{j \in N_i} \|\tilde{\omega}_j\|_1^2 \right) \right] \\ &= \sum_{i=1}^n \left[ -s_i^T K_i s_i - \left( \tilde{c}_{i,0} + \tilde{c}_{i,1} \sum_{j \in N_i} \|\tilde{\omega}_j\|_1 + \tilde{c}_{i,2} \sum_{j \in N_i} \|\tilde{\omega}_j\|_1^2 \right) \|s_i\|_1 \right] \end{aligned} \quad (23)$$

Taking the first derivative of  $V_2$  and making use of the parameter adaptation law (15) yields

$$\begin{aligned}\dot{V}_2 &= \sum_{i=1}^n (\kappa_{i,0}^{-1} \tilde{c}_{i,0} \dot{\tilde{c}}_{i,0} + \kappa_{i,1}^{-1} \tilde{c}_{i,1} \dot{\tilde{c}}_{i,1} + \kappa_{i,2}^{-1} \tilde{c}_{i,2} \dot{\tilde{c}}_{i,2}) \\ &= - \sum_{i=1}^n \left[ \left( \tilde{c}_0 + \tilde{c}_1 \sum_{j \in N_i} \|\tilde{\omega}_j\|_1 + \tilde{c}_2 \sum_{j \in N_i} \|\tilde{\omega}_j\|_1^2 \right) \|s_i\|_1 \right]\end{aligned}\quad (24)$$

Adding the above equation to Eq. (23) leads to

$$\dot{V} \leq - \sum_{i=1}^n s_i^T K_i s_i \leq 0 \quad (25)$$

Therefore, it follows that  $s_i \in \mathcal{L}^\infty$ , and  $\tilde{c}_{i,0}$ ,  $\tilde{c}_{i,1}$ , and  $\tilde{c}_{i,2} \in \mathcal{L}^\infty$ . Consequently, from Eq. (16) and Assumption 2, it is obtained that  $u_i \in \mathcal{L}^\infty$ . It follows that  $\dot{\tilde{\omega}}_i$ ,  $\dot{q}_i$ , and hence  $\dot{s}_i$  are all bounded from Eqs. (1) and (2). Integrating  $\dot{V}$  gives the results that  $s_i \in \mathcal{L}^2$ . Hence, using the corollary of Barbalat's lemma, it follows that  $\lim_{t \rightarrow \infty} s_i(t) = 0$  ( $i = 1, \dots, n$ ). Thus,  $\lim_{t \rightarrow \infty} S(t) = 0$ .  $\square$

**Remark 2:** There is no assumption on interspacecraft communication topology in the proposed control law. Thus, the proposed control law is applicable to any communication topology and is not restricted to be ring topology or undirected communication topology. The stability of the proposed control law is guaranteed even when there is no communication link, then each spacecraft will be controlled individually.

**Remark 3:** Unlike [8,10], there is no additional restriction on parameters  $b_i$  and  $a_{ij}$  other than  $b_i > 0$ ,  $a_{ij} \geq 0$  in Eq. (16). So the proposed attitude synchronization and tracking scheme will allow the designer to prioritize between station-keeping behavior and formation-keeping behavior. For example, if one wants to prioritize formation-keeping behavior,  $a_{ij}$  should be chosen to be large relative to  $b_i$ .

**Remark 4:** In the proposed control law, the desired attitude of each spacecraft with respect to inertial frame  $I$  is not restricted to be the same. Thus, the desired relative attitude between spacecraft can be maintained.

**Remark 5:** The proposed control law is discontinuous across the surface  $S(t)$ , thus leading to control chattering. This situation can be remedied by smoothing out the control discontinuity in a thin boundary layer neighboring the switching surface [23]. To do this, the sign function in the control law (16) can be replaced by a saturation function, which is defined as

$$\text{sat}(x) = \begin{cases} 1 & \text{if } \frac{x}{\phi} \geq 1 \\ \frac{x}{\phi} & \text{if } -1 < \frac{x}{\phi} < 1 \\ -1 & \text{if } \frac{x}{\phi} \leq -1 \end{cases}$$

where  $\phi$  is the boundary-layer thickness. The practical advantages of control law with this boundary layer may be significant, although it leads to small terminal tracking error. However, it should be pointed out that in this case the estimated gains  $\tilde{c}_{i,0}$ ,  $\tilde{c}_{i,1}$ , and  $\tilde{c}_{i,2}$  in Eq. (15) may become unbounded in the boundary layer, since the restriction to the sliding surface cannot always be achieved. To address this problem, the adaptive sliding-mode control law given in Eq. (16) is modified as

$$\begin{aligned}u_i &= -h_i + \left( \sum_{j=1, j \neq i}^n a_{ij} + b_i \right)^{-1} \left[ \sum_{j=1, j \neq i}^n a_{ij} (u_j + h_j) \right. \\ &\quad \left. - K_i s'_i - \hat{b}_i \text{sat}(s_i) \right], \quad i = 1, \dots, n\end{aligned}\quad (26)$$

where  $\text{sat}(s_i) \triangleq [\text{sat}(s_{i,1}), \text{sat}(s_{i,2}), \text{sat}(s_{i,3})]^T$ , with  $s'_i = [s'_{i,1}, s'_{i,2}, s'_{i,3}]^T$  and  $s'_{i,j} = s_{i,j} - \phi \text{sat}(s_{i,j})$  ( $i = 1, \dots, n$  and  $j = 1, 2, 3$ ), a measure of the algebraic distance of the current state to the boundary layer [23].

The adaptation laws (15) are modified as

$$\begin{aligned}\dot{\tilde{c}}_{i,0} &\triangleq \kappa_{i,0} \|s'_i\|_1 & \dot{\tilde{c}}_{i,1} &\triangleq \kappa_{i,1} \|s'_i\|_1 \sum_{j \in N_i} \|\tilde{\omega}_j\|_1 \\ \dot{\tilde{c}}_{i,2} &\triangleq \kappa_{i,2} \|s'_i\|_1 \sum_{j \in N_i} \|\tilde{\omega}_j\|_1^2\end{aligned}\quad (27)$$

Following [23], the convergence to the boundary layer can be easily shown. As seen from Eq. (27), the adaptation ceased as soon as the boundary layer is reached. This avoids the undesirable long-term drift found in many adaptive schemes and provides a consistent rule on when to cease adaptation.

#### IV. Illustrative Example

Simulation results are presented in this section to illustrate the performance and stability characteristics of the proposed decentralized sliding-mode control law. Two scenarios with four spacecraft are considered in the simulation. In the first scenario, the four spacecraft communicate via a directed line topology as shown in Fig. 1a, while a ring topology, shown in Fig. 1b, is used in the second scenario. Note that although both communication graphs have a spanning tree, the proposed control law is valid even when there is no spanning tree. The corresponding weighted Laplacian matrices for the topologies are

$$L_a = \begin{bmatrix} 1 & -1 & 0 & 0 \\ 0 & 1 & -1 & 0 \\ 0 & 0 & 1 & -1 \\ 0 & 0 & 0 & 0 \end{bmatrix} \quad L_b = \begin{bmatrix} 1 & -1 & 0 & 0 \\ 0 & 1 & -1 & 0 \\ 0 & 0 & 1 & -1 \\ -1 & 0 & 0 & 1 \end{bmatrix}$$

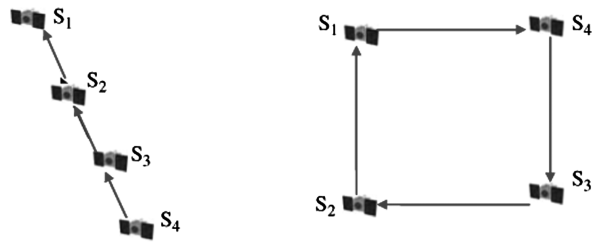
The actual inertia matrices of the spacecraft are assumed to be as follows (with unit expressed in  $\text{kg} \cdot \text{m}^2$ ):

$$\begin{aligned}J_1 &= \begin{bmatrix} 20 & 2 & 0.9 \\ 2 & 17 & 0.5 \\ 0.9 & 0.5 & 15 \end{bmatrix}, & J_2 &= \begin{bmatrix} 22 & 1 & 0.9 \\ 1 & 19 & 0.5 \\ 0.9 & 0.5 & 15 \end{bmatrix} \\ J_3 &= \begin{bmatrix} 18 & 1 & 1.5 \\ 1 & 15 & 0.5 \\ 1.5 & 0.5 & 17 \end{bmatrix}, & J_4 &= \begin{bmatrix} 18 & 1 & 1 \\ 1 & 20 & 0.5 \\ 1 & 0.5 & 15 \end{bmatrix}\end{aligned}$$

To validate the robustness of the proposed control law against model uncertainties and external disturbances, the nominal inertia matrices of the spacecraft are assumed to be

$$\bar{J}_1 = \bar{J}_2 = \bar{J}_3 = \bar{J}_4 = \text{diag}([20, 20, 20]^T) \text{ kg} \cdot \text{m}^2$$

and different sinusoidal-wave disturbances as in Eq. (28) are introduced to each spacecraft:



a) Line topology for in-track\in-plane formation      b) Ring topology for circular-like formation

Fig. 1 Interspacecraft directed communication topology.

$$\begin{aligned}
z_1(t) &= [0.10 \sin(0.4t), 0.05 \cos(0.5t), 0.08 \cos(0.7t)]^T \text{ Nm} \\
z_2(t) &= [0.06 \cos(0.4t), 0.10 \sin(0.5t), 0.05 \sin(0.7t)]^T \text{ Nm} \\
z_3(t) &= [0.08 \sin(0.4t + \pi/4), 0.06 \cos(0.5t + \pi/4), \\
&\quad 0.07 \cos(0.7t + \pi/4)]^T \text{ Nm} \\
z_4(t) &= [0.06 \cos(0.4t + \pi/4), 0.08 \sin(0.5t + \pi/4), \\
&\quad 0.10 \sin(0.7t + \pi/4)]^T \text{ Nm}
\end{aligned} \tag{28}$$

The external disturbances used in the simulation are far worse than those observed in practice.

The initial angular velocity errors of all spacecraft are chosen to be zeros, and the initial attitude-tracking errors are chosen as

$$\begin{aligned}
\bar{q}_1(0) &= [0.8986 \quad 0.4 \quad -0.1 \quad 0.15]^T, \\
\bar{q}_2(0) &= [0.8888 \quad -0.2 \quad 0.1 \quad 0.4]^T, \\
\bar{q}_3(0) &= [0.8062 \quad 0.1 \quad -0.5 \quad 0.3]^T, \\
\bar{q}_4(0) &= [0.8426 \quad -0.4 \quad -0.2 \quad 0.3]^T
\end{aligned}$$

The initial desired quaternions are  $\bar{\eta}_i^d(0) = [1 \quad 0 \quad 0 \quad 0]^T$  ( $i = 1, 2, 3, 4$ ). The time-varying desired angular velocities of the spacecraft are identical and given by Eq. (29). Then, the desired quaternions can be generated by using the attitude kinematic equations and Eq. (29):

$$\begin{aligned}
\omega_i^d(t) &= [0.1 \cos(t/10) \quad -0.1 \sin(t/10) \quad -0.1 \cos(t/10)]^T \\
i &= 1, 2, 3, 4
\end{aligned} \tag{29}$$

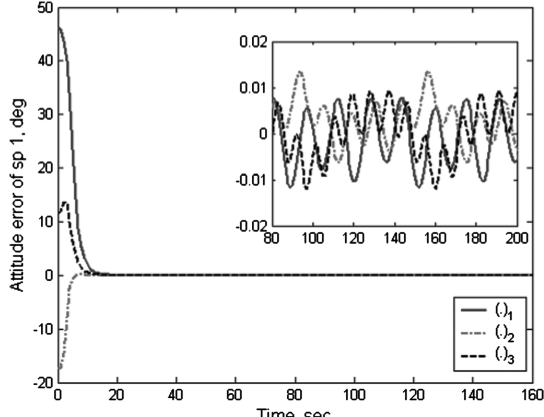


Fig. 2 Attitude tracking error of the first spacecraft.

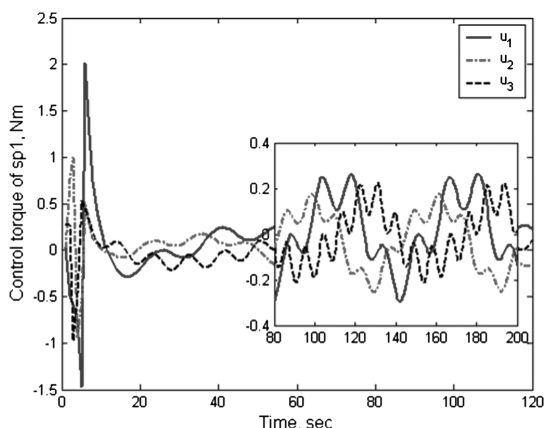


Fig. 3 Control torque of the first spacecraft.

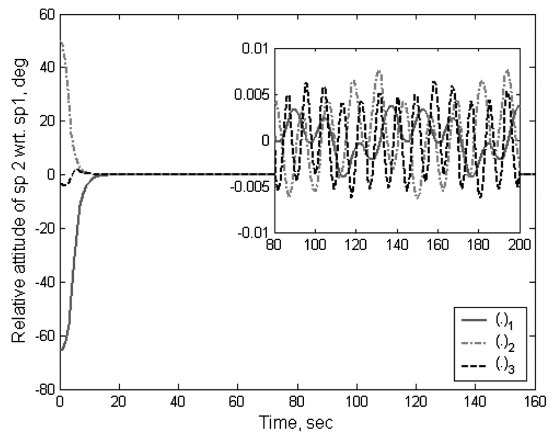


Fig. 4 Relative attitude error between the first and the second spacecraft.

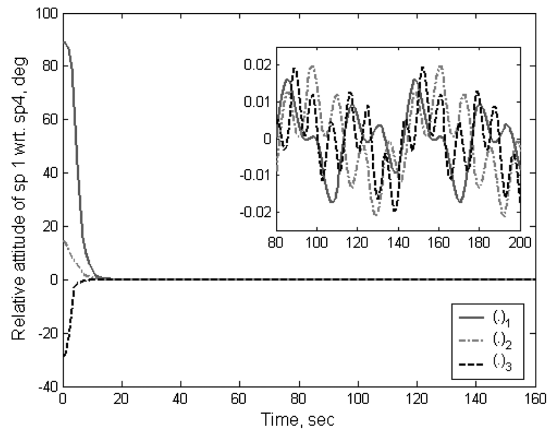


Fig. 5 Relative attitude error between the fourth and the first spacecraft.

#### A. Scenario 1: Line Communication Topology

The controller parameters in the first scenario are chosen with  $C = I_3$ ,  $b_i = 1$ ,  $\phi = 0.1i$ , and  $K_i = 0.01I_3$ , and the parameters of the adaptation law (27) are chosen with  $\bar{k}_{i,0} = 0.1$ ,  $\bar{k}_{i,1} = \bar{k}_{i,2} = 0.2$  ( $i = 1, \dots, 4$ ), and  $\hat{c}_{i,0}^0 = \hat{c}_{i,1}^0 = \hat{c}_{i,2}^0 = 0$ , where  $\hat{c}_{i,0}^0$ ,  $\hat{c}_{i,1}^0$ , and  $\hat{c}_{i,2}^0$  are the initial values of  $\hat{c}_{i,0}$ ,  $\hat{c}_{i,1}$ , and  $\hat{c}_{i,2}$ , respectively.

Figures 2 and 3 show the respective attitude errors and control torques of the first spacecraft using the control law, respectively. For ease of interpretation, attitude errors are expressed in Euler angles converted from unit quaternion. Attitude errors and control torques of the other spacecraft are similar to those of the first spacecraft and

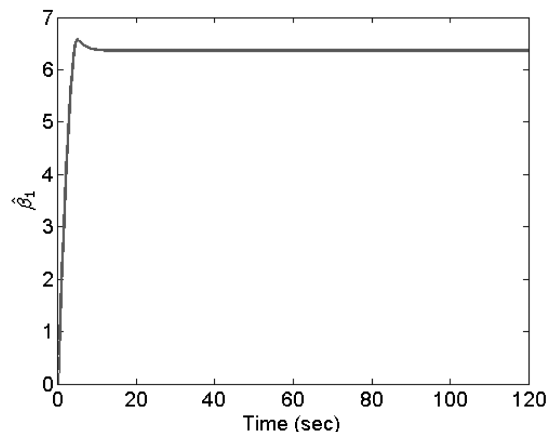


Fig. 6 Adaptive parameter  $\hat{\beta}_1$  of the first spacecraft.

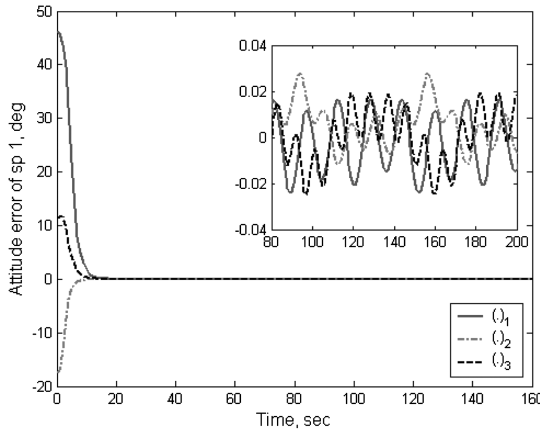


Fig. 7 Attitude tracking error of the first spacecraft without coupling between neighbors.

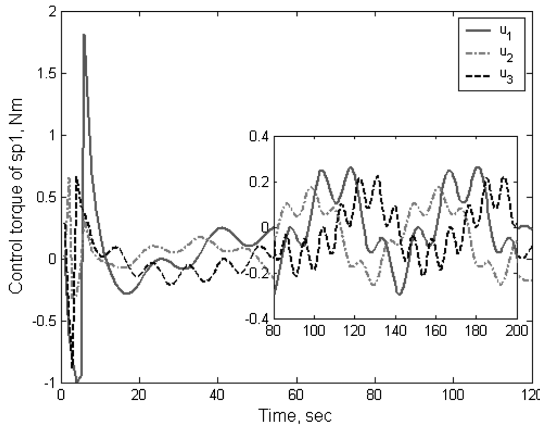


Fig. 8 Control torque of the first spacecraft without coupling between neighbors.

are not plotted here due to space constraint. Figures 4 and 5 show relative attitude errors between the first and second spacecraft and between fourth and first spacecraft, respectively. Relative attitude errors between other pairs of spacecraft are similar to those of the above two. The adaptive parameter  $\hat{\beta}_1$  defined in Eq. (17) with the control law (26) is bounded as shown in Fig. 6, and thus the efficacy of our proposed adaptation law (27) is verified. For comparison, Figs. 7–9 show attitude errors, control torques and relative attitude errors when there is no coupling between neighbors [i.e.,  $a_{ij} = 0$  ( $i, j = 1, 2, 3, 4$ ) in Eq. (26)]. As observed from simulation results,

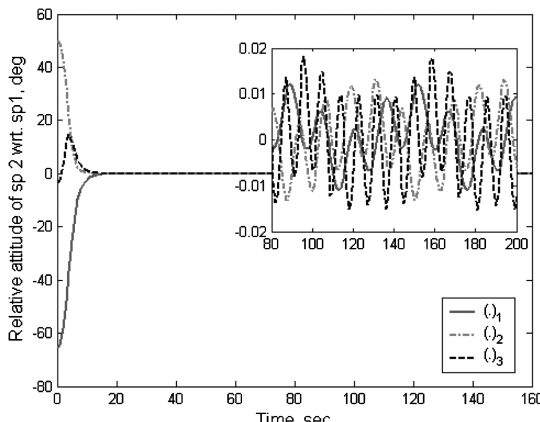


Fig. 9 Relative attitude error between the first and the second spacecraft without coupling between neighbors.

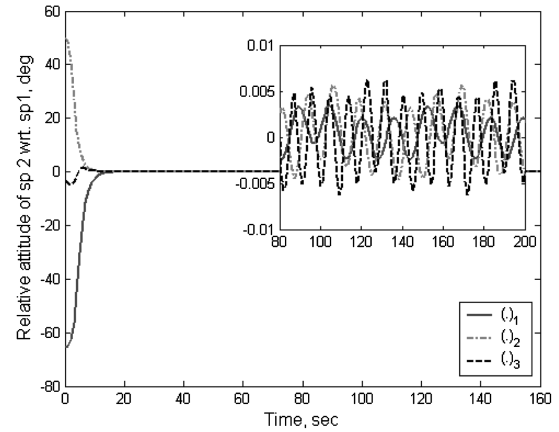


Fig. 10 Relative attitude error between the first and the second spacecraft under the ring topology.

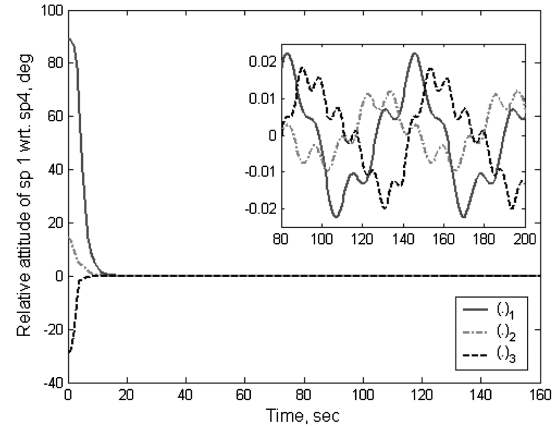


Fig. 11 Relative attitude error between the fourth and the first spacecraft under the ring topology.

relative attitude errors between spacecraft, especially the steady-state values, in the case with coupling between neighbors are smaller as compared with the case without coupling. Note that the magnitudes of steady-state control torques for the two cases are almost identical, as can be seen from Figs. 3 and 8.

#### B. Scenario 2: Ring Communication Topology

All the controller parameters in the second scenario are identical to those in the first scenario, except that  $a_{41} = 1$  in the second scenario. Figures 10 and 11 show relative attitude errors between the first and second spacecraft and between fourth and first spacecraft, respectively. As observed from Figs. 4, 5, 10, and 11, relative attitude errors in the ring topology are slightly smaller than those in the line topology, because additional coupling between fourth to first spacecraft is introduced in the ring topology. Thus, the simulation results validate the effectiveness of the proposed control law under a unidirectional ring communication topology.

## V. Conclusions

In this Note, the attitude synchronization and tracking problem in spacecraft formation under a general directed communication topology is addressed using unit quaternion parameterization. A decentralized adaptive sliding-mode control law is designed by introducing appropriate multispacecraft sliding-mode vector, which includes attitude error and angular velocity error of individual spacecraft, as well as relative attitude errors and relative angular velocity errors between spacecraft. An adaptive mechanism to estimate the model uncertainty and external disturbance bound was presented. Convergence of the tracking errors was established using

graph theoretic formulation. Numerical simulations are performed to validate the robust performance of the proposed control law in the presence of model uncertainties and disturbances. Simulation results demonstrate that each individual spacecraft converges to the desired attitude and angular velocity with acceptable control magnitude. Furthermore, relative attitude errors between spacecraft, especially the steady-state values, are reduced by including the relative attitude errors and relative angular velocity errors in the proposed control law.

### Acknowledgment

Funded in part under Project Agreement no. POD0513235 with Defense Science & Technology Agency and under Project Agreement no. DSOCL10004 with Defense Science Organization National Laboratories, Singapore.

### References

- [1] Wang, P. K. C., Hadaegh, F. Y., and Lau, K., "Synchronized Formation Rotation and Attitude Control of Multiple Free-Flying Spacecraft," *Journal of Guidance, Control, and Dynamics*, Vol. 22, No. 1, 1999, pp. 28–35.  
doi:10.2514/2.4367
- [2] Kang, W., and Yeh, H. H., "Co-Ordinated Attitude Control of Multi-Satellite Systems," *International Journal of Robust and Nonlinear Control*, Vol. 12, Nos. 2–3, 2002, pp. 185–205.  
doi:10.1002/rnc.682
- [3] Subbarao, K., and Welsh, S., "Nonlinear Control of Motion Synchronization for Satellite Proximity Operations," *Journal of Guidance, Control, and Dynamics*, Vol. 31, No. 5, 2008, pp. 1284–1294.  
doi:10.2514/1.34248
- [4] Kristiansen, R., Loria, A., Chaillet, A., and Nicklasson, P. J., "Spacecraft Relative Rotation Tracking without Angular Velocity Measurements," *Automatica*, Vol. 45, No. 3, 2009, pp. 750–756.  
doi:10.1016/j.automatica.2008.10.012
- [5] Beard, R., Lawton, J., and Hadaegh, F., "A Coordination Architecture for Spacecraft Formation Control," *IEEE Transactions on Control Systems Technology*, Vol. 9, No. 6, 2001, pp. 777–790.  
doi:10.1109/87.960341
- [6] Ren, W., and Beard, R. W., "Decentralized Scheme for Spacecraft Formation Flying via the Virtual Structure Approach," *Journal of Guidance, Control, and Dynamics*, Vol. 27, No. 1, Jan.–Feb. 2004, pp. 73–82.  
doi:10.2514/1.9287
- [7] Lawton, J., and Beard, R. W., "Synchronized Multiple Spacecraft Rotations," *Automatica*, Vol. 38, No. 8, 2002, pp. 1359–1364.  
doi:10.1016/S0005-1098(02)00025-0
- [8] VanDyke, M. C., and Hall, C. D., "Decentralized Coordinated Attitude Control Within a Formation of Spacecraft," *Journal of Guidance, Control, and Dynamics*, Vol. 29, No. 5, Sept.–Oct. 2006, pp. 1101–1109.  
doi:10.2514/1.17857
- [9] Chung, S.-J., Ahsun, U., and Slotine, J.-J. E., "Application of Synchronization to Formation Flying Spacecraft: Lagrangian Approach," *Journal of Guidance, Control, and Dynamics*, Vol. 32, No. 2, Mar.–Apr. 2009, pp. 512–526.  
doi:10.2514/1.37261
- [10] Jin, E. D., Jiang, X. L., and Sun, Z. W., "Robust Decentralized Attitude Coordination Control of Spacecraft Formation," *Systems and Control Letters*, Vol. 57, 2008, pp. 567–577.  
doi:10.1016/j.sysconle.2007.12.006
- [11] Abdessameud, A., and Tayebi, A., "Attitude Synchronization of a Group of Spacecraft Without Velocity Measurements," *IEEE Transactions on Automatic Control*, Vol. 54, No. 11, 2009, pp. 2642–2648.  
doi:10.1109/TAC.2009.2031567
- [12] Bai, H., Arcak, M., and Wen, J. T., "Rigid Body Attitude Coordination without Inertial Frame Information," *Automatica*, Vol. 44, 2008, pp. 3170–3175.  
doi:10.1016/j.automatica.2008.05.018
- [13] Dimarogonas, D. V., Tsiotras, P., and Kyriakopoulos, K. J., "Leader-Follower Cooperative Attitude Control of Multiple Rigid Bodies," *Systems and Control Letters*, Vol. 58, 2009, pp. 429–435.  
doi:10.1016/j.sysconle.2009.02.002
- [14] Ren, W., "Formation Keeping and Attitude Alignment for Multiple Spacecraft Through Local Interactions," *Journal of Guidance, Control, and Dynamics*, Vol. 30, No. 2, March–April 2007, pp. 633–638.  
doi:10.2514/1.25629
- [15] Ren, W., "Distributed Cooperative Attitude Synchronization and Tracking for Multiple Rigid Bodies," *IEEE Transactions on Control Systems Technology*, Vol. 18, No. 2, March 2010, pp. 383–392.  
doi:10.1109/TCST.2009.2016428
- [16] Fax, J. A., and Murray, R. M., "Information Flow and Cooperative Control of Vehicle Formations," *IEEE Transactions on Automatic Control*, Vol. 49, No. 9, Sept. 2004, pp. 1465–1476.  
doi:10.1109/TAC.2004.834433
- [17] Khoo, S. Y., Xie, L. H., and Man, Z. H., "Robust Finite-Time Consensus Tracking Algorithm for Multirobot Systems," *IEEE/ASME Transactions on Mechatronics*, Vol. 14, No. 2, 2009, pp. 219–228.  
doi:10.1109/TMECH.2009.2014057
- [18] Boskovic, J. D., Li, S. M., and Mehra, R. K., "Robust Tracking Control Design for Spacecraft Under Control Input Saturation," *Journal of Guidance, Control, and Dynamics*, Vol. 27, No. 4, 2004, pp. 627–633.  
doi:10.2514/1.1059
- [19] Merris, R., "Laplacian Matrices of Graphs: A Survey," *Linear Algebra and Its Applications*, Vol. 197, No. 198, 1994, pp. 143–176.  
doi:10.1016/0024-3795(94)90486-3
- [20] Horn, R., and Johnson, C., *Topics in Matrix Analysis*, Cambridge Univ. Press, Cambridge, England, U.K., 1991, pp. 242–254.
- [21] Lo, S.-C., and Chen, Y.-P., "Smooth Sliding-Mode Control for Spacecraft Attitude Tracking Maneuvers," *Journal of Guidance, Control, and Dynamics*, Vol. 18, No. 6, 1995, pp. 1345–1349.  
doi:10.2514/3.21551
- [22] Crassidis, J. L., Vadali, S. R., and Markley, F. L., "Optimal Variable-Structure Control Tracking of Spacecraft Maneuvers," *Journal of Guidance, Control, and Dynamics*, Vol. 23, No. 3, 2000, pp. 564–566.  
doi:10.2514/2.4568
- [23] Slotine, J. J. E., and Coetsee, J. A., "Adaptive Sliding Controller Synthesis for Non-Linear Systems," *International Journal of Control*, Vol. 43, 1986, pp. 1631–1651.  
doi:10.1080/00207178608933564